THE JOURNAL OF BIOLOGICAL CHEMISTRY VOL. 289, NO. 19, pp. 12989–12999, May 9, 2014

Up-regulation of Cholesterol Absorption Is a Mechanism for Cholecystokinin-induced Hypercholesterolemia*

Received for publication, November 11, 2013, and in revised form, March 20, 2014 Published, JBC Papers in Press, April 1, 2014, DOI 10.1074/jbc.M113.534388

LiChun Zhou[1], **Hong Yang**[1], **Emmanuel U. Okoro, and Zhongmao Guo**[2]

From the Department of Physiology, Meharry Medical College, Nashville, Tennessee 37208

Background: Intravenous injection of cholecystokinin (CCK) elevated mouse plasma cholesterol level.
Results: CCK enhances cholesterol absorption in mice and cultured cells. Inhibition of CCK receptors and their downstream signaling proteins diminishes CCK-induced cholesterol absorption.
Conclusion: Activation of enterocyte CCK receptors accelerates cholesterol absorption and induces hypercholesterolemia.
Significance: Inhibition of CCK receptors could be a therapeutic strategy for treatment of hypercholesterolemia.

Excessive absorption of intestinal cholesterol is a risk factor for atherosclerosis. This report examines the effect of cholecystokinin (CCK) on plasma cholesterol level and intestinal cholesterol absorption using the *in vivo* models of C57BL/6 wild-type and low density lipoprotein receptor knock-out ($LDLR^{-/-}$) mice. These data were supported by *in vitro* studies involving mouse primary intestinal epithelial cells and human Caco-2 cells; both express CCK receptor 1 and 2 (CCK1R and CCK2R). We found that intravenous injection of [Thr^{28},Nle^{31}]CCK increased plasma cholesterol levels and intestinal cholesterol absorption in both wild-type and $LDLR^{-/-}$ mice. Treatment of mouse primary intestinal epithelial cells with [Thr^{28},Nle^{31}]CCK increased cholesterol absorption, whereas selective inhibition of CCK1R and CCK2R with antagonists attenuated CCK-induced cholesterol absorption. In Caco-2 cells, CCK enhanced CCK1R/CCK2R heterodimerization. Knockdown of both CCK1R and CCK2 or either one of them diminished CCK-induced cholesterol absorption to the same extent. CCK also increased cell surface-associated NPC1L1 (Niemann-Pick C1-like 1) transporters but did not alter their total protein expression. Inhibition or knockdown of NPC1L1 attenuated CCK-induced cholesterol absorption. CCK enhanced phosphatidylinositide 3-kinase (PI3K) and Akt phosphorylation and augmented the interaction between NPC1L1 and Rab11a (Rab-GTPase-11a), whereas knockdown of CCK receptors or inhibition of G protein $\beta\gamma$ dimer ($G\beta\gamma$) diminished CCK-induced PI3K and Akt phosphorylation. Inhibition of PI3K and Akt or knockdown of PI3K diminished CCK-induced NPC1L1-Rab11a interaction and cholesterol absorption. Knockdown of Rab11a suppressed CCK-induced NPC1L1 translocation and cholesterol absorption. These data imply that CCK enhances cholesterol absorption by activation of a pathway involving CCK1R/CCK2R, $G\beta\gamma$, PI3K, Akt, Rab11a, and NPC1L.

An increase in plasma cholesterol, especially that pool of cholesterol carried by apolipoprotein B (apoB)-containing lipoproteins, has been suggested as a risk factor for the development of atherosclerosis (1). The apoB-carrying lipoproteins chylomicron and very low density lipoprotein (VLDL) are produced in the intestine and the liver, respectively (2). These circulating lipoproteins are partially metabolized by lipoprotein lipases, generating particles known as chylomicron remnants and low density lipoprotein (LDL). The LDL and chylomicron remnants are removed from the circulation mainly by an endocytic process mediated by hepatic LDL receptors (LDLRs)[3] and LDLR-related proteins. An increase in the generation of chylomicrons and/or VLDL and/or a decrease in the removal of LDL/chylomicron remnants would induce hypercholesterolemia.

Absorption of cholesterol from the intestine involves multiple processes (3, 4). Specifically, free cholesterol in the intestinal lumen is transported into enterocytes by the cholesterol transporter NPC1L1 (Niemann-Pick C1-like 1) (5). The internalized free cholesterol can be esterified by ACAT2 (acyl-CoA:cholesterol acyltransferase), forming esterified cholesterol, which is then transferred to chylomicrons by the microsomal triglyceride transport protein. Alternatively, free cholesterol can be exported by ATP-binding cassette A1 in the basolateral membrane and incorporated with apoAI to form high density lipoproteins (HDLs). The amount of intestinal cholesterol absorbed into the bloodstream varies from 20 to 80% among individuals (6). It has been shown that a change in the expression and/or activities of the aforementioned proteins alters the efficacy of enterocytes to absorb cholesterol (4).

A recent report from our laboratory showed that intravenous injection of [Thr^{28},Nle^{31}]cholecystokinin (CCK) significantly elevated the plasma cholesterol level in fasting low density lipoprotein receptor knock-out ($LDLR^{-/-}$) mice (7). Ligation of the bile duct, blocking CCK receptors with proglumide, or inhibition of the Niemann-Pick C1-like 1 transporter with ezetimibe reduced the hypercholesterolemic effect of CCK on $LDLR^{-/-}$ mice (7). These findings suggest that CCK increased plasma cholesterol as a result of promoting reabsorption of biliary cholesterol from the intestine.

* This work was supported, in whole or in part, by National Institutes of Health Grants R01HL089382 (to Z. G.) and SC1HL101431 (to H. Y.).
[1] Both authors contributed equally to this work.
[2] To whom correspondence should be addressed. Tel.: 615-327-6804; E-mail: zguo@mmc.edu.
[3] The abbreviations used are: LDLR, low density lipoprotein receptor; CCK, cholecystokinin; MPIEC, mouse primary intestinal epithelial cell; CCK1R and CCK2R, CCK receptor 1 and 2, respectively; Nle, norleucine; SI, sucrase isomaltase; RIP, Rab11-interacting protein; GAP, GTPase-activating protein.

The present report examines the regulatory role of CCK on intestinal cholesterol absorption using both mouse models and cultured cells. Our data demonstrate that intravenous injection of CCK significantly enhances intestine absorption of radioactive cholesterol in both wild-type and *LDLR*$^{-/-}$ mice. Mouse primary intestinal epithelial cells (MPIECs) and human colonic adenocarcinoma Caco-2 cells express both CCK receptor 1 (CCK1R) and CCK2R. Our data suggest that CCK enhances cholesterol absorption by activation of these two isoforms of CCK receptors. Data from Caco-2 cells suggest that CCK-induced cholesterol absorption is associated with activation of the G protein $\beta\gamma$ dimer ($G\beta\gamma$), phosphatidylinositide 3-kinase (PI3K), Akt, Rab-GTPase-11a (Rab11a), and NPLC1lL1. Further, inhibition or knockdown of these proteins diminishes CCK-induced transcellular cholesterol transport, suggesting a mechanistic role for them in CCK-induced cholesterol absorption.

EXPERIMENTAL PROCEDURES

Chemicals and Reagents—Caco-2 cells were purchased from ATCC. [Thr^{28},Nle^{31}] CCK was purchased from AnaSpec Inc. CCK1R antagonist lorglumide, CCK2R antagonist L365260 (L-4795), CCK2R agonist pentagastrin (B1636), G protein $\beta\gamma$ dimer inhibitor gallein (G1137), sodium cholate, sodium deoxycholate, lysophosphatidylcholine, and monopalmitoyl glycerol were purchased from Sigma-Aldrich. The CCK2R agonist A71236 was purchased from Torcris Bioscience. Ezetimibe was purchased from Selleck Chemicals LLC. Protein A/G Plus-agarose, Akt inhibitor XI (sc221229), scrambled (sc37007) and NPC1L1 siRNA (sc61225); Rab11a siRNAs (sc36340); PI3K p85α siRNA (sc36217); horseradish peroxidase- and fluorescein isothiocyanate-conjugated second antibodies (sc2314, sc2020, and sc2010); and primary antibodies against human NPC1L1 (sc166802), Rab11a (sc58465), phosphorylated Akt (sc7985-R), cytochrome P450 1a1 (CYP1a1) (sc9828), sucrase isomaltase (SI) (sc-393424), and CCK1R (sc43670) were purchased from Santa Cruz Biotechnology. CCK2R siRNA (H00000887-R02) was purchased from Abnova. The high capacity cDNA reverse transcription kit was purchased from Applied Biosystems. EZ-Link Sulfo-NHS-Biotin and biotinylation kits were obtained from Thermo Scientific. PI3K inhibitor 2-(4-morpholinyl)-8-phenyl-4H-1- benzopyran-4-one (LY294002) and phosphorylated PI3K antibody (catalog no. 4228) were obtained from Cell Signaling. [1,2-^{3}H]Cholesterol was obtained from PerkinElmer Life Sciences. The polyvinylidene difluoride (PVDF) membrane was obtained from Millipore. The ECL-plus chemiluminescence reagent was purchased from GE Healthcare. Fugene HD reagent and Opti-MEM medium were purchased from Promega and Invitrogen, respectively. Cholesterol assay kits were purchased from Modern Laboratory Services Inc. Transwell polycarbonate membrane cell culture inserts (catalog no. 3415) were obtained from Corning. Dulbecco's modified Eagle's medium (DMEM) and fetal bovine serum (FBS) were purchased from Invitrogen.

In Vivo Cholesterol Absorption—Male wild-type (C57BL/6) and *LDLR*$^{-/-}$ mice were obtained from the Jackson Laboratory and fed a chow diet containing ~5% fat and 19% protein by weight (Harlan Teklad). At ~4 months of age, mice were starved overnight and placed into one of two different but related studies. In the first study, wild-type and *LDLR*$^{-/-}$ mice were injected with either 50 ng/kg [Thr^{28},Nle^{31}]CCK or 50 μl of phosphate-buffered saline (PBS) via the tail vein under ketamine anesthesia as described previously (7). About 20 μl of blood was collected by retro-orbital bleeding before and 2 h after the injection of CCK. In the second study, wild-type and *LDLR*$^{-/-}$ mice were first injected with either 50 ng/kg [Thr^{28},Nle^{31}]CCK or 50 μl of PBS via the tail vein as above but were then gavage-fed with 0.1 μCi of [^{3}H]cholesterol (8); 2 h after the injection of CCK, ~0.5 ml of blood was collected via cardiac puncture under anesthesia. The mouse livers were perfused with PBS through the portal vein, and the livers were collected for determining absorbed radioactive cholesterol. All procedures were approved by the Institutional Animal Care and Use Committee at Meharry Medical College.

Plasma cholesterol was measured by spectrophotometric quantification using reagents obtained from Modern Laboratory Services (7). Plasma was fractionated by fast protein liquid chromatography (FPLC). The radioactivity in the liver, plasma, and FPLC fractions was determined by liquid scintillation counting (9). The radioactivity in various lipoproteins was calculated using the FPLC fractions, as we described previously (7, 9).

Cholesterol Micelles Preparation—A mixture containing 1.4 mM sodium cholate, 1.5 mM sodium deoxycholate, 1.7 mM phosphatidylcholine, 1.9 mM monopalmitoylglycerol, 2.2 mM oleic acid, and 0.02 μCi of [^{3}H]cholesterol or 0.1 μM unlabeled cholesterol was dissolved in chloroform/methanol (1:1, v/v) (10) and dried using a Labconco CentriVap concentrator. The pellet was resuspended in an equal volume of DMEM by sonication. The micellar solution was passed through a 0.20-μm filter and kept at 37 °C until use. The micelle stock was diluted 10 times with DMEM for treatment of cells.

Cholesterol Association and Secretion in MPIECs—MPIECs were isolated using an EDTA treatment method (8). Briefly, the jejunum and ileum obtained from wild-type mice were cleaned with a washing solution containing 117 mM NaCl, 5.4 mM KCl, 0.96 mM NaH_2PO_4, 26.19 mM $NaHCO_3$, and 5.5 mM glucose and then filled with the washing solution supplemented with 1.5 mM EDTA and 0.5 mM dithiothreitol. The intestine was bathed in oxygenated 0.9% NaCl at 37 °C for 10 min. The luminal contents were collected and centrifuged at 1,500 × *g* for 5 min. The cell pellet was resuspended in 1 ml of DMEM supplemented with 10% FBS in a 6-well plate and cultured at 37 °C for 30 min. The purity of the isolated cells was examined by flow cytometry (FACSCalibur, BD Biosciences) after the cells were sequentially stained with a primary antibody against the enterocyte marker protein SI and a FITC-conjugated second antibody. About 86% of the cells were SI-positive. Trypan blue staining repeatedly demonstrated that ~90% of the isolated cells remain viable, and the viability was not changed within 6 h (data not shown).

To study the effect of CCK on cholesterol association, MPIECs were treated for 10 min with 10 nM [Thr^{28},Nle^{31}]CCK with or without 1 μM lorglumide or L365260. Thereafter, 100 μl of a 0.02-μCi [^{3}H]cholesterol micellar solution was added to the culture and incubated for an additional 5, 10, 15, 30, or 60 min.

Radioactivity associated with the cells was determined by liquid scintillation counting. To study the effect of CCK on cholesterol secretion, MPIECs were first incubated with the [^{3}H]cholesterol micellar solution for 1 h as described above. After removal of the [^{3}H]cholesterol micellar solution, cells were incubated in fresh DMEM for an additional 2 h in the presence or absence of CCK with or without lorglumide or L365260 as described above. The radioactivity in the enterocyte-conditioned medium was counted for determination of cholesterol secretion. The [^{3}H]cholesterol micellar solution was generated following the method described by Iqbal *et al.* (10).

Caco-2 Cell Cultures—Caco-2 cells were seeded in 6.5- and 24-mm transwell inserts and cultured in 24- and 6-well plates in DMEM supplemented with 20% FBS for 21 days. The medium in the apical and basolateral compartments was then replaced, respectively, with 10% FBS and 0.5% bovine serum albumin (BSA), unless otherwise stated.

Transcellular Cholesterol Transport in Caco-2 Cells—Caco-2 cells grown in transwell inserts were cultured in 24-well plates. Transcellular cholesterol transport was determined as described by Iqbal *et al.* (10), with brief modifications. Specifically, the apical medium was replaced with 200 μl of 0.002-μCi [^{3}H]cholesterol micelles solution supplemented with 10% FBS. The basolateral medium was replaced with 1.2 ml of 5% BSA with or without 10 nM CCK, 100 nM A71623, or 100 pM pentagastrin. In experiments using CCK antagonists or G protein $\beta\gamma$ dimer, PI3K and Akt inhibitors, 50 nM lorglumide, 200 nM L365260, 10 μM gallein (11), 20 μM LY294002, or 600 nM Akt inhibitor XI was added into the basolateral medium. After an 18-h incubation, the basolateral-conditioned medium was centrifuged at 13,000 $\times$ *g* for 10 min. The supernatant was filtrated through a 0.2-μm PVDF membrane by using a Bio-Rad microfiltration blotting device to eliminate the cholesterol that was not associated with lipoprotein. The radioactivity on the membrane was determined by liquid scintillation analysis for determination of transcellularly transported [^{3}H]cholesterol.

Small Interfering RNA (siRNA) Knockdown—Caco-2 cells seeded in transwell inserts were transfected with scrambled siRNA or specific siRNA against CCK1R, CCK2R, or Rab11a using Fugene HD reagent and Opti-MEM medium according to the manufacturer's instructions. After 6 h, cells were replenished with fresh medium containing 10% FBS and cultured for an additional 24 h. These transfection procedures were repeated one more time (12). In the experiments for determination of protein levels, transfected cells grown in 24-mm transwell inserts were treated with 10 nM CCK or DMEM alone (control) in the basolateral compartment for time periods as indicated in the figure legends and harvested for Western blot analysis. In the experiments for determination of cholesterol absorption, transfected cells grown in 6.5-mm transwell inserts were incubated for 18 h with 0.002 μCi of [^{3}H]cholesterol micelles in the apical compartment and 10 nM CCK or DMEM alone as a control. The radioactivity in the basolateral medium was determined by liquid scintillation analysis.

Immunoprecipitation and Biotin Precipitation—Caco-2 cells grown in transwell inserts were treated with 10 nM CCK or DMEM (control) in the basolateral compartment for 1 h. In the experiments involving PI3K and Akt inhibitors, cells were incubated with 10 μM gallein, 20 μM LY294002, or 600 nM Akt inhibitor XI for 30 min prior to CCK treatment. For immunoprecipitation, the cells were lysed with a lysis buffer containing 50 mM Tris HCl (pH 8), 150 mM NaCl, 1% Triton, 2 mM EDTA, and a proteinase inhibitor mixture. A 20-μl aliquot of the cell lysate was taken for input control in Western blot analysis. The rest of the lysate was incubated with protein A/G Plus-agarose beats on ice for 1 h (13). The agarose was removed by centrifugation at 2,000 $\times$ *g* for 5 min. Precleaned lysates were incubated with antibodies against Rab11a, CCK1R, or CCK2R at 4 °C for 2 h and then incubated with Protein A/G Plus-agarose beads at 4 °C for 14 h. The pelleted beads were washed once with lysis buffer and then three times with washing buffer (lysis buffer minus Triton) and resuspended in Western blot loading buffer. The agarose beads were discarded by centrifugation at 10,000 $\times$ *g* for 1 min.

For biotin precipitation of membrane proteins, the cells treated with CCK with or without LY294002 or Akt inhibitor XI were incubated with the Sulfo-NHS-Biotin reagent in the apical side at 4 °C for 2 h (14). After the cells were lysed, a 20-μl aliquot of lysate was taken for an input control in a Western blot analysis. The rest of the lysate was incubated with Streptavidin-agarose at 4 °C for 45 min. The pelleted beads were washed once with lysis buffer and then three times with washing buffer and resuspended in Western loading buffer. The agarose beads were discarded by centrifugation at 10,000 $\times$ g for 1 min. The biotin precipitants were analyzed by Western blots with NPC1L1, SI, or CYP1a1 antibodies. SI is highly expressed in the apical membrane and used as an apical marker protein in Caco-2 cells (15), whereas CYP1a1 is expressed mainly in the cytosol and endoplasmic reticulum (16).

Western Blot Analysis—Caco-2 cells were treated as described for the immunoprecipitation and biotin precipitation studies. Cells were lysed in M-PER mammalian protein extraction reagent. Cell lysates as well as the immunoprecipitated and biotin-precipitated proteins were resolved on 10% SDS-polyacrylamide gels. The proteins were transferred to a PVDF membrane. After blocking with 5% fat-free milk, the membranes were incubated with antibodies as indicated in the figure legends. Immunoreactive bands were visualized using ECL-plus chemiluminescence reagent (GE Healthcare) and analyzed with a GS-700 Imaging Densitometer (Bio-Rad) (16).

Quantitative Real-time RT-PCR Assay—Caco-2 cells grown in a transwell insert were treated with 10 nM CCK or culture medium alone in the basolateral compartment for the time periods indicated in the figure legends. Total RNA was extracted using TRIzol reagent and subjected to reverse transcription using a high capacity cDNA reverse transcription kit (Applied Biosystems). The resulting cDNAs were subjected to quantitative real-time PCR with an iCycler system (Bio-Bad) using primers synthesized by Qiagen for amplification of NPC1L1, CCK1R, CCK2R, and glyceraldehyde 3-phosphate dehydrogenase (GAPDH) (16). The specific primers used for amplification of these genes are presented in Table 1.

The expression level of CCK1R and CCK2R mRNAs was determined as described by Jin *et al.* (17) with a slight modification. Briefly, standard CCK1R and CCK2R cDNA fragments were synthesized using the primers described above. The PCR

TABLE 1
Primers used for real-time RT-PCR

Genes	Sequence (5′–3′)
Human NPC1L1	
Forward	CCGCAGAGCTTCTGTGTATCC
Reverse	TATCTTCCCTGGTTCCGAACGAC
Human GAPDH	
Forward	GAGCCAAAAGGGTCATCATC
Reverse	TAAGCAGTTGGTGGTGCAGG
Human CCK1R	
Forward	GGAACTCTACCAGGGAATAA
Reverse	GCATGCGGATCACCCTTTTC
Human CCK2R	
Forward	GACACGAGAATTGGAGCTGG
Reverse	CAAAGATGAATGTGCCCATGAG
Mouse CCK1R	
Forward	ATCCCTGTCCCGGTATTCCTAC
Reverse	CAGTCCCCTCCTTTCTGCTG
Mouse CCK2R	
Forward	CAACAAATGTGGTCCGTGCT
Reverse	GGTCTCGCTGTCATTATCACC

products generated using Caco-2 cell cDNA as a template included 242 and 224 bp of CCK1R and CCK2R cDNAs, respectively, whereas the PCR products from MPE cDNA included 97 and 135 bp of CCK1R and CCK2R cDNAs, respectively. The molar concentration of the cDNA products was calculated on the basis of their absorbance values and molecular weights. The cDNA products were serially diluted to prepare standard cDNA solutions and subjected to PCR amplification as per test samples (17). Standard curves for each standard cDNA were constructed by plotting the cDNA concentration (fM) *versus* the PCR threshold cycle (C_t) (*i.e.* the fraction cycle number at which a PCR product was first detected). The concentration of the mRNA in the test samples was determined by fitting the measured C_t to the standard curve. The level of the CCK1R and CCK2R mRNAs in Caco-2 cells and MPIECs was expressed relative to the total cellular protein level.

Statistical Analysis—Data are reported as the mean ± S.E. Differences between treatment and control groups were analyzed by Student's unpaired *t* test or analysis of variance followed by Tukey's post hoc test. Statistical significance was considered when *p* was less than 0.05. Statistix software was used for statistical analyses.

RESULTS

CCK Elevates Plasma Cholesterol Levels and Accelerates Intestinal Cholesterol Absorption in Mice—Plasma CCK concentrations have been reported to be 1.5–10 pM in mice (18–20) and 1.2–26 pM in humans at the fasting state (21, 22) and elevate from 50% to 400% after a meal. We previously reported that the fasting plasma CCK concentrations were 10.7 ± 0.9 and 11.7 ± 1.2 pM in 4-month-old male wild-type and *LDLR*$^{-/-}$ mice, respectively (7). The CCK concentrations in these mice were elevated ~30% at 30 min after injection of 50 ng/kg [Thr^{28},Nle^{31}]CCK and returned to the basal level 2 h after injection (7). We also observed that the plasma cholesterol levels in CCK-treated wild-type and *LDLR*$^{-/-}$ mice were ~13 and 31% higher, respectively, than their vehicle-treated controls (7). Similarly, data from this report show that the plasma cholesterol level was elevated by ~21 and 37% in wild-type and

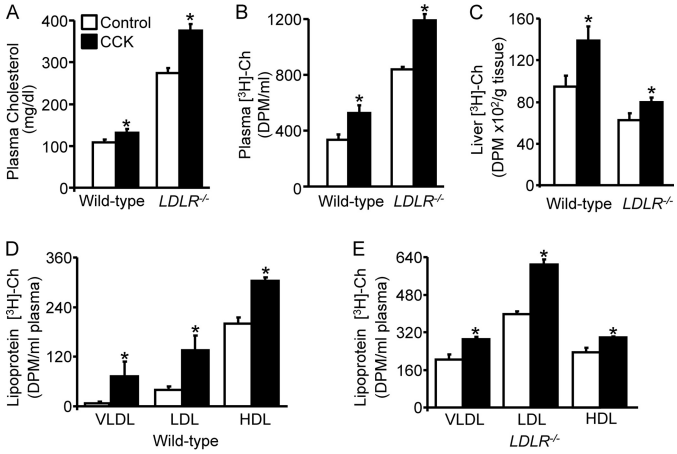

FIGURE 1. **CCK increases plasma cholesterol levels and intestinal cholesterol absorption in mice.** *A*, blood samples were collected by retro-orbital bleeding from wild-type and *LDLR*$^{-/-}$ mice before (control) and 2 h after injection of 50 ng/kg of [Thr^{28},Nle^{31}]CCK via the tail vein. *B–E*, wild-type and *LDLR*$^{-/-}$ mice were gavage-fed 1 μCi of [^{3}H]cholesterol and injected with 50 ng/kg [Thr^{28},Nle^{31}]CCK or 200 μl of PBS (control) via the tail vein. Blood and liver samples were collected at 2 h postinjection. Plasma was fractionated with an FPLC system. Plasma cholesterol levels (*A*) were determined by spectrophotometric quantification. Radioactivity in the plasma (*B*) and the liver (*C*) as well as in the VLDL, LDL, and HDL fractions (*D* and *E*) was determined by liquid scintillation counting. Values represent the means ± S.E. (*error bars*) ($n = 15$ mice/group in plasma cholesterol studies and $n = 5$/group in cholesterol absorption studies). *, $p < 0.05$ *versus* controls.

LDLR$^{-/-}$ mice, respectively, after an intravenous injection of 50 ng/kg [Thr^{28},Nle^{31}]CCK (Fig. 1*A*). These results suggest that CCK is able to elevate plasma cholesterol in mouse models, and the hypercholesterolemic activity of CCK is more prominent in *LDLR*$^{-/-}$ mice than in wild-type mice. To study the mechanism responsible for an apparent CCK-induced hypercholesterolemia, we examined the impact of CCK on intestine cholesterol absorption by measuring the plasma and liver radioactivity following a [^{3}H]cholesterol tracer dose fed by gavage. Data in Fig. 1, *B* and *C*, show that the radioactivity in the plasma was significantly higher in CCK-treated mice than in untreated control mice. This suggests that the CCK-induced hypercholesterolemia results, at least in part, from an increase in intestinal cholesterol absorption. In addition, the plasma radioactivity was significantly higher in *LDLR*$^{-/-}$ mice than in wild-type mice, whereas the accumulated radioactivity in the liver was significantly higher in wild-type mice than in *LDLR*$^{-/-}$ mice under both CCK-treated and control conditions. Because the liver is the primary organ for removal of LDL and chylomicron remnants from the plasma, a reduced clearance of remnant lipoproteins by the liver might account for the stronger hypercholesterolemic effect of CCK in *LDLR*$^{-/-}$ mice than in wild-type mice.

The plasma cholesterol in wild-type mice is distributed mostly in HDL, whereas knockout of LDLR mainly elevates LDL and VLDL cholesterol (7, 23). The data in Fig. 1, *D* and *E*, illustrate that the plasma radioactivity was distributed mainly to the HDL fraction in wild-type mice and to the LDL/VLDL fractions in *LDLR*$^{-/-}$ mice. These findings are consistent with the distribution of cholesterol in lipoproteins in wild-type mice and *LDLR*$^{-/-}$ mice. Fig. 1, *D* and *E*, also shows that CCK increases radioactive cholesterol in all of the lipoprotein fractions. Specifically, intravenous injection of 50 ng/kg

[Thr^{28},Nle^{31}]CCK to WT mice increased the VLDL, LDL, and HDL radioactivity by 65, 95, and 104 dpm/ml of plasma, respectively (Fig. 1*D*). The same dose of CCK increased VLDL, LDL, and HDL radioactivity by 85, 210, and 58 dpm/ml plasma, respectively, in *LDLR*$^{-/-}$ mice (Fig. 1*E*). These data suggest that the greater hypercholesterolemic effect of CCK in *LDLR*$^{-/-}$ mice than in wild-type mice results mainly from accumulation of absorbed cholesterol in the LDL fraction.

CCK Enhances Transcellular Cholesterol Transport in Caco-2 Cells by Activation of Both CCK1R and CCK2R—The Caco-2 cell line has been used as a tissue culture model for intestinal absorption (5, 24). These cells spontaneously form polarized cell monolayers in culture that exhibit many of the morphological and functional characteristics of normal enterocytes, including the production and polarized secretion of lipoproteins synthesized from absorbed lipids (24). We observed that Caco-2 cells expressed CCK1R and CCK2R, with a greater expression of CCK2R. Specifically, the amounts of CCK1R and CCK2R mRNAs were 2.3 ± 0.3 and 18.2 ± 1.4 fM/g of cellular proteins, respectively. The protein level of CCK2R was also ~1.9-fold higher than CCK1R in Caco-2 cells. The data in Fig. 2, *A* and *B*, showed that CCK1R and CCK2R can be co-immunoprecipitated by antibodies against their isoforms and that CCK treatment increases the amount of the co-immunoprecipitated receptor. For example, the levels of CCK2R protein precipitated by CCK1R antibody and the CCK1R protein precipitated by CCK2R antibody were ~2.3- and 2.5-fold higher, respectively, in cells treated with CCK for 2 min than in those without CCK treatment. Prolongation of CCK treatment to 15 min slightly elevated the amount of precipitated CCK receptors; however, the difference of the precipitated proteins between 2 and 15 min did not reach statistical significance. The immunoblotting images of the input controls in Fig. 2*A* illustrate that CCK treatment did not affect the cellular expression level of these receptors. These results suggest that CCK1R and CCK2R form heterodimers in Caco-2 cells and that binding with CCK enhances their heterodimerization.

This study determined the impact of CCK on cholesterol absorption using Caco-2 cells as a model of the intestinal barrier. The dose-response curve in Fig. 2*C* shows that the transcellular transport of [^{3}H]cholesterol was increased ~46% when [Thr^{28},Nle^{31}]CCK was raised from 1 to 10 nM, with no further rise at higher CCK concentrations. It has been suggested that intestinal cholesterol is absorbed by formation of both chylomicrons and HDL (8). We next studied the effect of CCK receptor agonists and antagonists on cholesterol absorption in Caco-2 cells. Fig. 2*D* shows that the CCK A71623 and pentagastrin mimicked the effect of CCK with regard to the stimulation of cholesterol absorption. Pentagastrin is ~968-fold selective for CCK2R over CCK1R (25), whereas A71623 is 1200-fold selective for CCK1R over CCK2R (26). The data in Fig. 2*D* also indicate that inhibition of CCK receptors by the CCK1R-preferring antagonist lorglumide or the CCK2R-preferring antagonist L365260 diminished CCK-induced cholesterol absorption. These findings were confirmed by knockdown of CCK receptors. Fig. 2, *E* and *F*, illustrates that transfection of Caco-2 cells with both CCK1R and CCK2R siRNAs or either one of them reduced CCK1R and/or CCK2R proteins by ~50–60%.

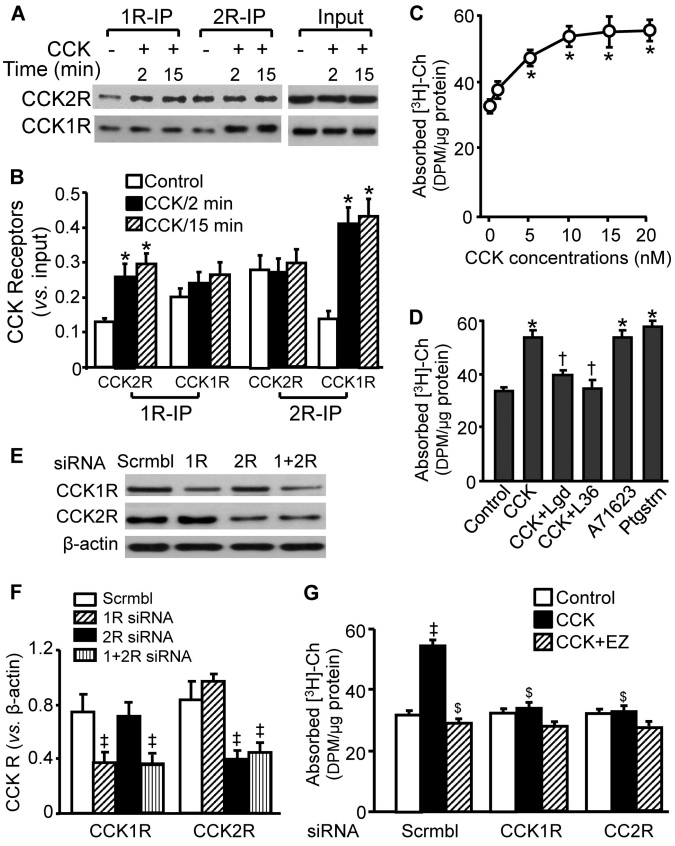

FIGURE 2. **CCK enhances cholesterol absorption in Caco-2 cells by activation of both CCK1R and CCK2R.** *A* and *B*, Caco-2 cells cultured in transwell inserts were treated with culture medium alone as a control or 10 nM [Thr^{28},Nle^{31}]CCK for 2 or 15 min. The protein extracts were subjected to immunoprecipitation. The products immunoprecipitated by antibodies against CCK1R (*1R-IP*) and CCK2R (*2R-IP*) were analyzed by Western blots. The precipitated CCK1R and CCK2R were expressed relative to the immunoblot intensity of its input control. *C*, Caco-2 cells grown in transwell inserts were incubated for 18 h with 0.002 μCi of [^{3}H]cholesterol (*[^{3}H]-Ch*) micelles in the apical compartment and with the indicated concentrations of [Thr^{28},Nle^{31}]CCK in the basolateral compartment. *D*, Caco-2 cells grown in transwell inserts were incubated for 18 h with 0.002 μCi of [^{3}H]cholesterol micelles in the apical compartment and with one of the following reagents or reagent combinations in the basolateral compartment: culture medium alone (*Control*), 100 nM A71623, 100 pM pentagastrin (*Ptgstrn*), or 10 nM [Thr^{28},Nle^{31}]CCK with or without 50 nM lorglumide (*Lgd*) or 200 nM L365260 (*L36*). *E* and *F*, Caco-2 cells were transfected with scrambled (*Scrmbl*) siRNA or siRNAs specific for CCK1R (*1R*), CCK2R (*2R*), or both CCK1R and CCK2R (*1 + 2R*). The protein levels of CCK1R and CCK2R were determined by Western blot analysis and expressed relative to β-actin. *G*, Caco-2 cells grown in transwell inserts were transfected with scrambled siRNA, or siRNA specific for CCK1R, CCK2R, or both CCK1 and CCK2R and then incubated with 0.002 μCi of [^{3}H]cholesterol micelles in the apical compartment and with culture medium alone (*Control*) or 10 nM [Thr^{28},Nle^{31}]CCK with or without 50 μM ezetimibe (*EZ*) in the basolateral compartment. Absorbed [^{3}H]cholesterol was determined by radioactivity counting of the basolateral medium. Values represent the mean ± S.E. (*error bars*) of 4–5 independent experiments. *, $p < 0.05$ *versus* control; †, $p < 0.05$ *versus* cells treated with CCK alone; ‡, $p < 0.05$ *versus* cells transfected with scrambled siRNA alone; $, $p < 0.05$ *versus* cells treated with scrambled siRNA and CCK.

Fig. 2*G* demonstrates that underexpression of either CCK1R or CCK2R or both of them significantly diminished CCK-induced cholesterol absorption. These data suggest that both CCK1R and CCK2R contribute to cholesterol absorption in Caco-2 cells.

The data in Fig. 2*G* also show that inhibition of the cholesterol transporter activity of NPC1L1 by ezetimibe suppressed CCK-induced cholesterol absorption in Caco-2 cells trans-

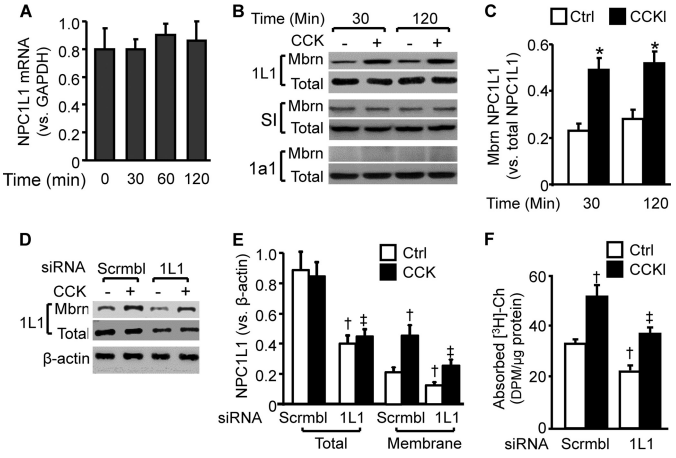

FIGURE 3. **CCK induces cholesterol absorption in Caco-2 cells by regulation of NPC1L1 protein membrane translocation.** *A*, Caco-2 cells grown in transwell inserts were treated with 10 nM [Thr^{28},Nle^{31}]CCK in the basolateral compartment for the indicated time periods. NPC1L1 mRNAs were determined with real-time RT-PCR and quantitated relative to the GAPDH mRNA level. *B* and *C*, Caco-2 cells grown in transwell inserts were treated with culture medium alone as a control (*ctrl*) or 10 nM [Thr^{28},Nle^{31}]CCK in the basolateral compartment for 30 or 120 min. *D* and *E*, Caco-2 cells were transfected with scrambled (*Scrmbl*) siRNA or siRNA specific for NPC1L1 and then treated with culture medium alone as a control or 10 nM [Thr^{28},Nle^{31}]CCK in the basolateral compartment for 30 min. Apical membrane proteins were isolated by biotin precipitation. NPC1L1 (*1L1*), SI, and CYP1a1 (*1a1*) proteins in the membrane and the total cell lysate were determined with Western blot analysis. The levels of membrane (*Mbrn*) and total NPC1L1 were expressed relative to the total level of β-actin. *F*, Caco-2 cells transfected with scrambled siRNA or siRNA specific for NPC1L1 were incubated with 0.002 μCi of [^{3}H]cholesterol micelles in the apical compartment and with culture medium alone (control) or 10 nM [Thr^{28},Nle^{31}]CCK in the basolateral compartment. Absorbed [^{3}H]cholesterol was determined by radioactivity counting of the basolateral medium. Values represent the mean ± S.E. (*error bars*) of five independent experiments. *, $p < 0.05$ *versus* cells incubated with medium alone (control); †, $p < 0.05$ *versus* cells with scrambled siRNA transfection and without CCK treatment; ‡, $p < 0.05$ *versus* cells with scrambled siRNA transfection and CCK treatment.

fected with scrambled control siRNA but did not induce further decrease in cholesterol absorption in cells transfected with CCK1R and/or CCK2R siRNAs. These findings imply that activations of CCK receptors and NPC1L1 are two essential steps in a pathway through which CCK induces cholesterol absorption. Inhibition of either of these two steps could diminish CCK-induced cholesterol absorption; however, simultaneous inhibition of both of them cannot cause greater suppressive effect than inhibition of one of them alone.

CCK Increases Membrane NPC1L1 in Caco-2 Cells—It is known that NPC1L1 is primarily located in recycling endosomes in the basal state (27, 28). Translocation of the NPC1L1 to the apical surface of enterocytes is a critical step in cholesterol absorption. Fig. 3, *A* and *B*, data show that treatment of Caco-2 cells with 10 nM [Thr^{28},Nle^{31}]CCK did not alter NPC1L1 total cellular protein and mRNA levels. However, this dose of CCK increased the membrane-associated NPC1L1 protein levels by ~2.1- and 2.3-fold at 30 and 120 min post-treatment, respectively (Fig. 3, *B* and *C*). In this study, cell surface membrane proteins were isolated by biotin precipitation. The purity of the isolated proteins was confirmed by the absence of the cytoplasmic protein CYP1a1 (16) and the presence of apical marker protein SI (15) in the precipitants (Fig. 3*B*).

This study determined the impact of underexpressing NPC1L1 on CCK-induced cholesterol absorption. Fig. 3, *D* and *E*, data show that transfection of Caco-2 cells with NPC1L1 siRNA reduced total NPC1L1 proteins by ~55 and 47%, respectively, in cells treated with or without CCK. CCK treatment did not alter the total NPC1L1 protein level in cells transfected with scrambled or NPC1L1 siRNA. In contrast, CCK significantly increased membrane NPC1L1 in these two lines of cells, whereas the protein levels of membrane NPC1L1 under the control conditions and after CCK treatment were ~41 and 46% less, respectively, in cells transfected with NPC1L1 siRNA than in those transfected with scrambled siRNA (Fig. 3, *D* and *E*). Furthermore, CCK significantly increased cholesterol absorption in these two lines of cells, whereas the levels of absorbed cholesterol under the control conditions and after CCK treatment also were ~33 and 28% less, respectively, in cells transfected with NPC1L1 siRNA than in those transfected with scrambled siRNA (Fig. 3*F*). These data suggest that the cholesterol absorption efficiency in Caco-2 cells is positively related to the NPC1L1 protein level in the cell surface. This suggests that CCK increases cholesterol absorption by promoting NPC1L1 translocation to the cell surface.

CCK Induces PI3K and Akt Phosphorylation in Caco-2 Cells—It has been suggested that the PI3K-Akt pathway regulates the recycling of vesicles to the cell surface (29). This experiment studied the impact of CCK on PI3K and Akt expression and phosphorylation. As shown in Fig. 4, *A* and *B*, CCK treatment did not alter the levels of total PI3K and Akt proteins but increased PI3K and Akt phosphorylation in a time-dependent manner. Specifically, CCK-induced PI3K phosphorylation started at 2 min post-treatment, reached a peak at 15 min, started to decline at 30 min, and returned to the basal level within 60 min. CCK-induced Akt phosphorylation occurred at 5 min after treatment, started to decline at ~60 min, and returned to the basal level within 120 min. Knockdown of CCK1R or CCK2R by siRNAs or inhibition of G protein βγ dimer (Gβγ) with gallein diminished CCK-induced PI3K and Akt phosphorylation (Fig. 4, *C*–*G*). It has been established that activation of CCK receptors triggers the PI3K-Akt pathway via the G protein βγ dimer (Gβγ). Data in Fig. 4, *C* and *D*, indicate that inhibition of Gβγ with gallein attenuated CCK-induced PI3K and Akt phosphorylation. In addition, inhibition of PI3K and Akt by LY294002 and Akt inhibitor XI, respectively, diminished the CCK-induced NPC1L1 translocation (Fig. 4*H*) and cholesterol absorption (Fig. 4*I*). These results indicate that CCK enhances PI3K and Akt phosphorylation by activation of Gβγ and both CCK1R and CCK2R and that activation of the PI3K-Akt pathway is a mechanism by which CCK induces NPC1L1 translocation and cholesterol absorption.

CCK Increases Rab11a-NPC1L1 Interactions in Caco-2 Cells—Translocation of NPC1L1 to the cell surface is mediated by a protein complex containing Rab11 and its effectors (30, 31). Activation of PI3K-Akt has been suggested as a means to increase the capability of Rab11 to drive recycling vesicle translocation to the cell surface (32). Here we studied the impact of CCK on the physical interaction of Rab11a with NPC1L1 in Caco-2 cells. The data in Fig. 5, *A and B*, indicate that NPC1L1 is co-immunoprecipitated with Rab11a. CCK treatment did not alter the expression levels of Rab11a and NPC1L1 proteins but increased the co-precipitated NPC1L1 by ~2.2-fold. Knock-

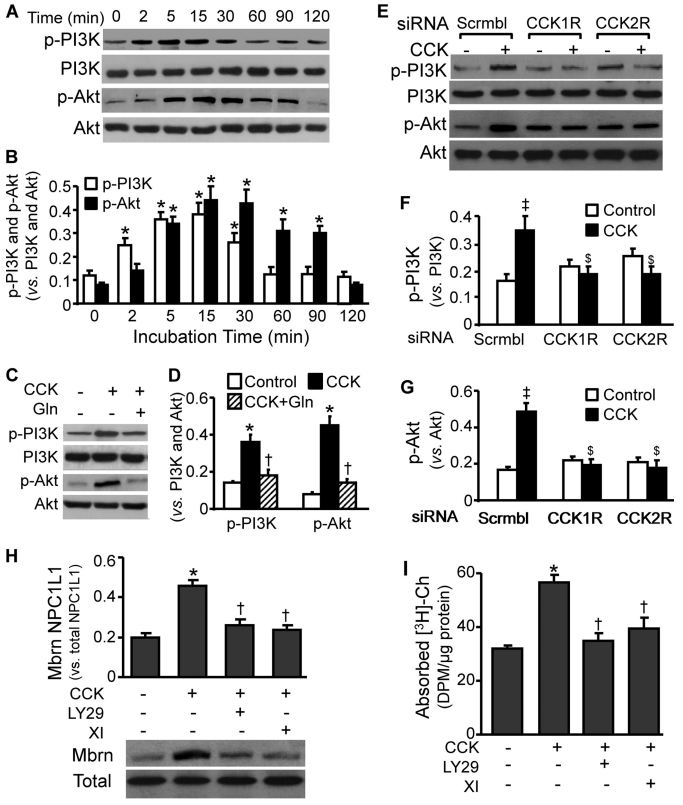

FIGURE 4. **CCK induces cholesterol absorption in Caco-2 cells by activation of a PI3K-Akt pathway.** *A* and *B*, Caco-2 cells grown in transwell inserts were treated with 10 nM [Thr^{28},Nle^{31}]CCK in the basolateral compartment for the indicated time periods. *C* and *D*, Caco-2 cells were treated with culture medium alone as a control or 10 nM [Thr^{28},Nle^{31}]CCK with or without 10 μM gallein for 15 min. *E–G*, Caco-2 cells were transfected with scrambled (*Scrmbl*) siRNA or siRNAs specific for CCK1R or CCK2R and then treated with 10 nM [Thr^{28},Nle^{31}]CCK or medium alone as a control in the basolateral compartment for 15 min. The protein levels of total and phosphorylated PI3K (*p-PI3K*) and Akt (*p-Akt*) were determined by Western blot analysis. *H*, Caco-2 cells were treated with culture medium alone or 10 nM [Thr^{28},Nle^{31}]CCK with or without 20 μM LY294002 (*LY29*) or 600 nM Akt inhibitor XI (*XI*) in the basolateral compartment at 37 °C for 30 min and then incubated with 2 mM Sulfo-NHS-Biotin reagent in the apical compartment at 4 °C for 2 h. Membrane proteins were precipitated with Pierce Streptavidin-agarose resins. Membrane (*Mbrn*) NPC1L1 was determined by Western blot analysis and expressed relative to total NPC1L1 levels. *I*, Caco-2 cells were incubated for 18 h with 0.002 μCi of [^{3}H]cholesterol ([^{3}*H*]-*Ch*) micelles in the apical compartment and culture medium alone or 10 nM [Thr^{28},Nle^{31}]CCK with or without 20 μM LY294002 or 600 nM Akt inhibitor XI in the basolateral compartment. Absorbed [^{3}H]cholesterol was determined by radioactivity counting of the basolateral medium. Values represent the mean ± S.E. (*error bars*) of five independent experiments. *, $p < 0.05$ *versus* control; †, $p < 0.05$ *versus* CCK treatment alone; ‡, $p < 0.05$ *versus* cells with scrambled siRNA transfection and without CCK treatment; $, $p < 0.05$ *versus* cells treated with scrambled siRNA and CCK.

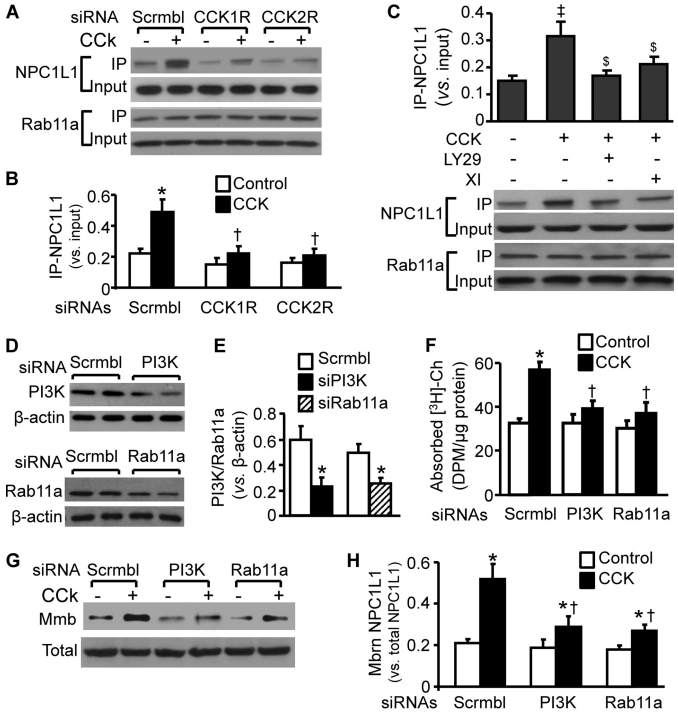

FIGURE 5. **Rab11a is involved in CCK-induced NPC1L1 translocation and cholesterol absorption.** *A* and *B*, Caco-2 cells were transfected with scrambled (*Scrmbl*) siRNA or siRNA specific for CCK1R or CCK2R and then were treated with 10 nM [Thr^{28},Nle^{31}]CCK in the basolateral compartment for 30 min. *C*, Caco-2 cells were treated with culture medium alone or 10 nM [Thr^{28},Nle^{31}]CCK with or without 20 μM LY294002 (*LY29*) or 600 nM Akt inhibitor XI (*XI*) in the basolateral compartment. Proteins were precipitated by a Rab11a antibody. The precipitants and input whole-cell lysates were analyzed by Western blots with antibodies against Rab11a and NPC1L1. Immunoprecipitated (*IP*) NPC1L1 was expressed relative to the immunoblot intensity of its input control. *D* and *E*, Caco-2 cells were transfected with scrambled siRNA or siRNA specific for PI3K (*siPI3K*) or Rab11a (*siRab11a*). The protein levels of PI3K and Rab11a were determined by Western blot analysis and expressed relative to β-actin. *F*, Caco-2 cells transfected with PI3K, Rab11a, or scrambled siRNAs were incubated for 18 h with 0.002 μCi of [^{3}H]cholesterol ([^{3}*H*]-*Ch*) micelles in the apical compartment and 10 nM [Thr^{28},Nle^{31}]CCK or culture medium alone (*control*) in the basolateral compartment. Absorbed [^{3}H]cholesterol was determined by radioactivity counting of the basolateral medium. *G* and *H*, Caco-2 cells transfected with PI3K, Rab11a, or scrambled siRNAs were treated with 10 nM [Thr^{28},Nle^{31}]CCK in the basolateral compartment for 30 min. Membrane proteins were isolated by biotin precipitation. NPC1L1 proteins in the membrane (*Mbrn*) and the total cell lysate were determined with Western blot analysis. The level of membrane NPC1L1 was expressed relative to its total protein level. Values represent the mean ± S.E. (*error bars*) of 4–5 independent experiments. *, $p < 0.05$ *versus* cells with scrambled siRNA transfection and without CCK treatment; †, $p < 0.05$ *versus cells* treated with scrambled siRNA and CCK; ‡, $p < 0.05$ *versus* medium incubation alone; $, $p < 0.05$ *versus* CCK treatment alone.

down of CCK1R or CCK2R reduced the amount of NPC1L1 co-precipitated with Rab11a in CCK-treated cells (Fig. 5, *A* and *B*). Fig. 5*C* shows that inhibition of PI3K or Akt by LY294002 and Akt inhibitor XI diminished CCK-induced Rab11a-NPC1L1 interaction. These results suggest that CCK enhances the physical interaction of Rab11a and NPC1L1 via activation of CCK1R/CCK2R, PI3K, and Akt.

Having demonstrated the interaction of Rab11a and NPC1L1, we then studied the regulatory role of Rab11a in CCK-induced NPLC1 translocation and cholesterol absorption by knockdown of Rab11a expression. Fig. 5, *D* and *E*, shows an ~56% reduction in Rab11a protein in cells transfected with Rab11a siRNA as compared with the cells transfected with scrambled control siRNAs. This level of Rab11a underexpression attenuated CCK-induced cholesterol absorption (Fig. 5*F*) and NPC1L1 translocation (Fig. 5, *G* and *H*). These suggest that Rab11a mediates NPC1L1 translocation to the cell surface (30, 31). Here we also confirmed the regulatory effect of PI3K on CCK-induced NPC1L1 translocation and cholesterol absorption by knockdown of PI3K. We observed that transfection of Caco-2 cells with siRNA specific for PI3K regulatory subunit p85α reduced the protein level of this gene by ~62% (Fig. 5, *D* and *E*). This level of PI3K underexpression did not significantly alter the basal level of NPC1L1 translocation and cholesterol absorption but decreased CCK-induced NPC1L1 translocation

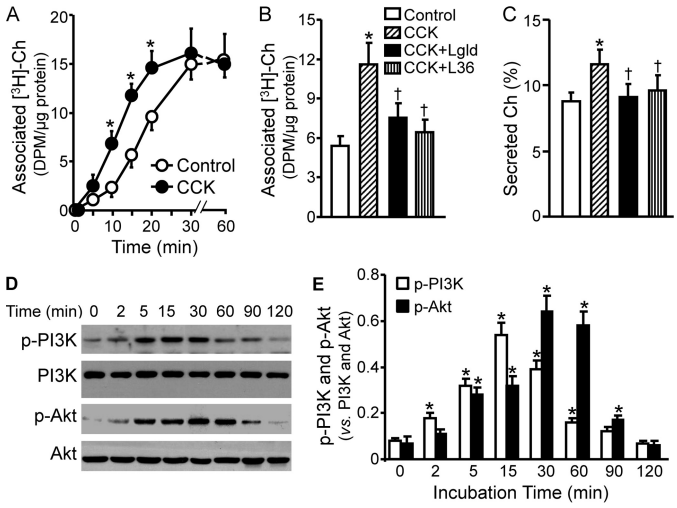

FIGURE 6. **CCK enhances cholesterol association and secretion in MPIECs.** *A* and *B*, MPIECs were treated in a 6-well plate with culture medium alone (*Control*) or 10 nM [Thr^{28},Nle^{31}]CCK (*A*) or 10 nM [Thr^{28},Nle^{31}]CCK with or without 50 nM lorglumide (*Lgd*) or 200 nM L365260 (L36) (*B*) for 10 min. Thereafter, 0.002 μCi of [^{3}H]cholesterol ([^{3}*H*]-*Ch*) micelles were added to the culture. After incubation for the additional time periods as indicated (*A*) or the 15-min time period (*B*), the radioactivity associated with cells was determined by liquid scintillation counting. *C*, MPIECs were incubated with 0.002 μCi of [^{3}H]cholesterol micelles for 1 h and then with a non-radioactive medium in the absence (*Control*) or presence of 10 nM [Thr^{28},Nle^{31}]-CCK with or without 50 nM lorglumide or 200 nM L365260 for an additional 2 h. The radioactivity in the enterocyte-conditioned medium was counted for the determination of cholesterol secretion measures (percentage). Values represent the mean ± S.E. (*error bars*) of five independent experiments. *D* and *E*, MPIECs were treated with 10 nM [Thr^{28},Nle^{31}]CCK for the indicated time periods. The protein levels of total and phosphorylated PI3K and Akt were determined by Western blot analysis. The level of phosphorylated PI3K and Akt was expressed relative to the level of total PI3K and Akt. *, $p < 0.05$ *versus* controls incubated for the same period of time; †, $p < 0.05$ *versus* CCK treatment alone.

and cholesterol absorption by ~67 and 75%, respectively (Fig. 5, *E* and *F*). This agrees with the finding in Fig. 4, *H* and *I*, that inhibition of PI3K by LY294002 diminished CCK-induced NPC1L1 translocation and cholesterol absorption.

CCK Enhances Cholesterol Association and Secretion and Induces PI3K and Akt Phosphorylation in MPIECs—Because of the difficulty of directly measuring transcellular cholesterol transport in a cellular suspension of MPIECs, this report studied the effect of CCK on cholesterol association with and secretion from these cells. Fig. 6*A* shows that cell-associated radioactivity increased with time. In the absence of CCK, cell-associated radioactivity reached a maximum value at 30 min after incubation with [^{3}H]cholesterol and remained at a plateau value thereafter. CCK treatment did not alter the maximum value of cell-associated radioactivity but accelerated the association of MPIECs with cholesterol. Specifically, CCK-treated cells achieved their maximum radioactivity association within 20 min and manifested a greater association at 10–20 min after incubation with [^{3}H]cholesterol compared with untreated control cells (Fig. 6*A*). Because the level of cell-associated radioactivity is a result of the equilibrium between cell uptake and secretion of [^{3}H]cholesterol, cholesterol uptake was dominant at the beginning of the incubation time, whereas cholesterol secretion increased as cholesterol accumulated within the cells. When cholesterol secretion came into balance with uptake, cell-associated radioactivity reached a maximum value and remained on a plateau. Thus, the ability of CCK to shorten the time period for achievement of the maximal radioactivity association and elevate the level of cell-associated radioactivity at the early incubation time periods suggests an up-regulatory effect of CCK on MPIEC cholesterol uptake. Pretreatment of MPIECs with the CCK receptor antagonist lorglumide or L365260 diminished the up-regulatory effect of CCK on cholesterol association in MPIECs (Fig. 6*B*). It has been reported that lorglumide is ~2,300-fold more selective for CCK1R over CCK2R, whereas L365260 is ~140-fold selective for CCK2R over CCK1R (25). Our data thus suggest that CCK enhances cholesterol association by activation of both CCK1R and CCK2R.

Secretion of internalized cholesterol across the basolateral membrane is another critical step of cholesterol absorption (8). The data in Fig. 6*C* show that treatment of MPIECs with 10 nM [Thr^{28},Nle^{31}]CCK elevated cholesterol secretion by 33% and that pretreatment of MPIECs with lorglumide or L365260 significantly diminished CCK-elevated cholesterol secretion in MPIECs. These data suggest that activation of CCK1R and CCK2R also enhances cholesterol secretion.

Similar to the results seen in Caco-2 cells, CCK treatment also induced a time-dependent increase in PI3K and Akt phosphorylation in MPIECs. Specifically, CCK-induced PI3K and Akt phosphorylation started at 2 and 5 min, respectively, and returned to the basal level within 90 and 120 min post-treatment, respectively (Fig. 6, *D* and *E*).

DISCUSSION

Results from our previous (7) and current studies are consistent in that they both demonstrate that intravenous injection of CCK elevates plasma cholesterol in wild-type and *LDLR*$^{-/-}$ mice and that the response is greater in *LDLR*$^{-/-}$ mice. The greater hypercholesterolemic effect of CCK in *LDLR*$^{-/-}$ mice appears to be due to a decreased clearance of plasma cholesterol by the liver. Specifically, we observed that a [^{3}H]cholesterol feeding-induced accumulation of radioactivity was higher in the plasma but lower in the liver in *LDLR*$^{-/-}$ mice than in wild-type mice; this was true under control and CCK treatment conditions. It has been known that absorbed cholesterol is removed from the plasma mainly by the liver and that the rate of hepatic LDL cholesterol clearance in wild-type mice (~500 ml/day/kg) is ~20-fold greater in *LDLR*$^{-/-}$ mice (~25 ml/day/kg) (33). Thus, it is highly likely that the high rate of hepatic LDL cholesterol clearance in wild-type mice forestalls accumulation of absorbed cholesterol in the plasma and therefore prevents hypercholesterolemia. It is worthwhile to note that the activity of human liver to clear remnant lipoprotein cholesterol is relatively low. Specifically, the rate of hepatic remnant lipoprotein clearance in humans (12 ml/day/kg) is ~40-fold less than in wild-type mice (33). In contrast, the rate of hepatic clearance of remnant lipoprotein cholesterol in *LDLR*$^{-/-}$ mice is only ~2-fold greater than in humans (33). It is therefore rational to postulate that CCK could induce an even greater rise in hypercholesterolemia in human subjects than in *LDLR*$^{-/-}$ mice, and the data obtained from *LDLR*$^{-/-}$ mice would be more physiologically relevant than those from wild-type mice. It has been reported that human plasma cholesterol and CCK concentrations as well as intestinal cholesterol absorption rates elevate

with age (34–36). Therefore, it will be interesting to determine whether an increase in plasma CCK is at least in part responsible for age-related hypercholesterolemia.

Enterocyte-mediated cholesterol uptake and secretion are essential steps for cholesterol transport across the intestinal epithelial cell barrier (8). This report demonstrates that mouse enterocytes express both CCK1R and CCK2R. Treatment of mouse enterocytes with CCK enhanced cholesterol uptake and secretion. Blockade of CCK1R or CCK2R with their antagonists attenuated the up-regulatory role of CCK on cholesterol uptake and secretion in these cells. These findings suggest that direct stimulation of enterocytes is a mechanism by which CCK enhances intestinal cholesterol absorption and that both CCK1R and CCK2R contribute to the regulatory activity of CCK in enterocyte cholesterol absorption. This concept is supported by the experimental data from Caco-2 cells, which also express both CCK1R and CCK2R. Treatment of Caco-2 cells with CCK and agonists selective for CCK1R or CCK2R enhanced transcellular cholesterol transport. Blockade of CCK1R or CCK2R with antagonists or knockdown of these receptors with siRNAs diminished CCK-induced transcellular cholesterol transport in Caco-2 cells. In addition, we observed that CCK stimulation induced CCK1R/CCK2R heterodimerization. It has been reported that CCK1R and CCK2R are able to form homo- and heterodimers (37, 38). Heterodimerization of these receptors enhances agonist-induced activities, such as cellular signaling and cell proliferation (38). It is highly likely that binding of CCK with CCK1R and/or CCK2R triggers heterodimerization of these receptors, activates the downstream signaling pathways, and enhances cholesterol absorption. Thus, underexpression of either CCK1R or CCK2R reduces the formation of the heterodimers and diminishes CCK-induced cholesterol absorption, whereas underexpression of both CCK1R and CCK2R will not induce greater suppressive effects than underexpression of either one of them alone.

This report also demonstrates that CCK increased cell surface NPC1L1 but did not alter the total NPC1L1 protein levels in Caco-2 cells. Under steady state conditions, NPC1L1 is located predominantly in transferrin-rich recycling vesicles in the perinuclear region (27, 28). Absorption of cholesterol requires translocation of NPC1L1 to the cell membrane, a process mediated by a protein complex containing Rab-GTPase-11 (Rab11) and its partner Rab11 family of interacting protein-2 (FIP2) (30, 31) or other Rab11-interacting proteins (RIPs), such as Rip11 and Rab-coupling protein (32). The data from this report document the regulatory role of Rab11a in CCK-induced NPC1L1 translocation and cholesterol absorption. Specifically, we observed that CCK enhanced the interaction between NPC1L1 and Rab11a and that knockdown of Rab11a inhibited CCK-induced NPC1L1 surface translocation and transcellular cholesterol transport in Caco-2 cells. These data suggest that CCK stimulation enhances the physical interaction of Rab11a and NPC1L1, resulting in NPC1L1 translocation and cholesterol absorption.

Two CCK receptor subtypes have been identified in mammalian cells (*i.e.* CCK1R and CCK2R) (39). Both of them are G-protein-coupled receptors. Stimulation of GPCRs, such as CCK receptors, is able to trigger a PI3K-dependent pathway via activation of $G\beta\gamma$ (40). In this pathway, the $G\beta\gamma$ dimer activates PI3K, which phosphorylates phosphoinositides to form phosphatidylinositol 3-phosphate and other phosphorylated phosphoinositides. These lipids bind both Akt and phosphoinositide-dependent protein kinase 1 (PDK1). This co-localization allows PDK1 to phosphorylate Akt (41). Indeed, data from this report demonstrate that activation of either CCK1R or CCK2R was able to activate the PI3K-Akt pathway (*i.e.* treatment of Caco-2 cells with CCK augmented PI3K and Akt phosphorylation, and knockdown of CCK1R or CCK2R or inhibition of the $G\beta\gamma$ dimer weakened CCK-induced PI3K and Akt phosphorylation).

Activation of the PI3K-Akt pathway has been suggested as a mechanism for activation of Rab11 complex and the sequential cell surface translocation of recycling vesicles (29). For instance, activation of PI3K-Akt pathway by insulin has been shown to induce phosphorylation of Rab GTPase-activating proteins (GAPs). The Akt-phosphorylated GAPs dissociate with the Rab11-RIP protein complex. This dissociation enables the GTP-bound form of Rab11 to drive the recycling vesicle translocation to the cell membrane (32). Insulin also has been shown to induce NPC1L1 translocation from recycling vesicles to the cell surface (28). The data from this report demonstrate that inhibition of PI3K or Akt diminished CCK-induced Rab11a-NPC1L1 interaction and NPC1L1 translocation and reduced CCK-induced transcellular cholesterol transport. These data suggest that activation of a PI3K-Akt pathway is a mechanism by which CCK activates Rab11a and induces NPC1L1 translocation to the cell surface, leading to cholesterol absorption. The data in this report also showed that the NPC1L1 protein level in the cell membrane continued to remain at a high level after 2 h of CCK treatment, whereas PI3K and Akt phosphorylation had returned to the basal level at this time point. Currently, the mechanism for triggering NPC1L1 relocation to the storage compartment from the cell surface remains unclear.

In summary, this report demonstrates that CCK increased cholesterol absorption *in vitro* and *in vivo*. Treatment of Caco-2 cells with CCK also induced NPC1L1 translocation, Rab11a-NPC1L1 interaction, and PI3K and Akt phosphorylation. Inhibition of CCK1R/CCK2R, Rab11a, PI3K, or Akt diminished CCK-induced NPC1L1 translocation and cholesterol absorption. In addition, CCK treatment enhanced CCK1R/CCK2R heterodimerization in Caco-2 cells. Based on the findings from the current work and the known functions of the above mentioned molecules (29, 32, 40, 41), we propose the following model to describe how CCK up-regulates cholesterol absorption (Fig. 7). CCK1R and CCK2R form heterodimers in response to ligand binding. Such a receptor complex triggers a pathway involving $G\beta\gamma$, PI3K, phosphatidylinositol 3-phosphate, PDK1, Akt, GAPs, and RIPs, which enhances the interaction of Rab11a with NPC1L1 and induces NPC1L1 translocation to the cell surface, leading to an increase in cholesterol absorption. Further studies are required to confirm the involvement of PDK1, GAPs, and RIPs in this CCK-activated pathway.

It is known that activation of G-protein-coupled receptors is able to activate other signaling pathways, such as the phospho-

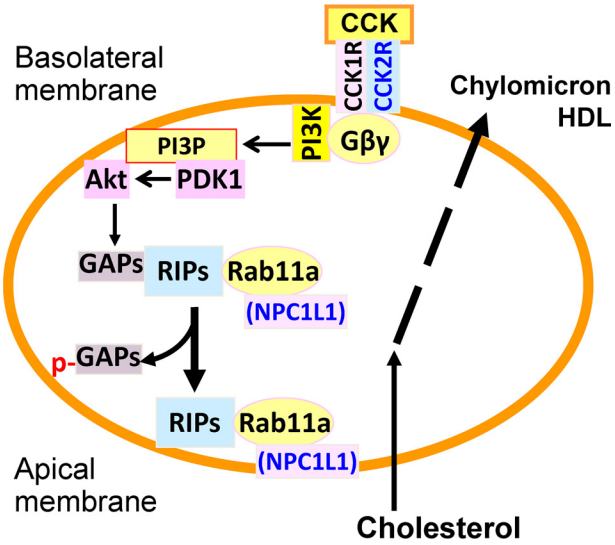

FIGURE 7. **Proposed mechanism for CCK-induced cholesterol absorption.**

lipase C-dependent pathway (42) and cyclic AMP-dependent pathway (43). Activation of CCK receptors has been shown to regulate cellular function through these pathways (43, 44). Further studies are required in order to understand if these pathways also contribute to CCK-induced cholesterol absorption.

Acknowledgment—We thank Dr. Diana Marver for critical reading of the manuscript.

REFERENCES

1. Rackley, C. E. (2000) Cardiovascular basis for cholesterol therapy. *Cardiol. Rev.* **8,** 124–131
2. Havel, R. J., and Hamilton, R. L. (2004) Hepatic catabolism of remnant lipoproteins: where the action is. *Arterioscler. Thromb. Vasc. Biol.* **24,** 213–215
3. Iqbal, J., and Hussain, M. M. (2009) Intestinal lipid absorption. *Am. J. Physiol. Endocrinol. Metab* **296,** E1183–E1194
4. Calandra, S., Tarugi, P., Speedy, H. E., Dean, A. F., Bertolini, S., and Shoulders, C. C. (2011) Mechanisms and genetic determinants regulating sterol absorption, circulating LDL levels, and sterol elimination: implications for classification and disease risk. *J. Lipid Res.* **52,** 1885–1926
5. Sané, A. T., Sinnett, D., Delvin, E., Bendayan, M., Marcil, V., Ménard, D., Beaulieu, J. F., and Levy, E. (2006) Localization and role of NPC1L1 in cholesterol absorption in human intestine. *J. Lipid Res.* **47,** 2112–2120
6. Repa, J. J., and Mangelsdorf, D. J. (2000) The role of orphan nuclear receptors in the regulation of cholesterol homeostasis. *Annu. Rev. Cell Dev. Biol.* **16,** 459–481
7. Zhou, L., Yang, H., Lin, X., Okoro, E. U., and Guo, Z. (2012) Cholecystokinin elevates mouse plasma lipids. *PLoS One* **7,** e51011
8. Iqbal, J., and Hussain, M. M. (2005) Evidence for multiple complementary pathways for efficient cholesterol absorption in mice. *J. Lipid Res.* **46,** 1491–1501
9. Wu, D., Yang, H., Xiang, W., Zhou, L., Shi, M., Julies, G., Laplante, J. M., Ballard, B. R., and Guo, Z. (2005) Heterozygous mutation of ataxia-telangiectasia mutated gene aggravates hypercholesterolemia in apoE-deficient mice. *J. Lipid Res.* **46,** 1380–1387
10. Iqbal, J., Anwar, K., and Hussain, M. M. (2003) Multiple, independently regulated pathways of cholesterol transport across the intestinal epithelial cells. *J. Biol. Chem.* **278,** 31610–31620
11. Lehmann, D. M., Seneviratne, A. M., and Smrcka, A. V. (2008) Small molecule disruption of G protein βγ subunit signaling inhibits neutrophil chemotaxis and inflammation. *Mol. Pharmacol.* **73,** 410–418
12. Lin, X., Yang, H., Zhang, H., Zhou, L., and Guo, Z. (2013) A novel transcription mechanism activated by ethanol: induction of Slc7a11 gene expression via inhibition of the DNA-binding activity of transcriptional repressor octamer-binding transcription factor 1 (OCT-1). *J. Biol. Chem.* **288,** 14815–14823
13. Chen, X., Guo, Z., Okoro, E. U., Zhang, H., Zhou, L., Lin, X., Rollins, A. T., and Yang, H. (2012) Up-regulation of ATP binding cassette transporter A1 expression by very low density lipoprotein receptor and apolipoprotein E receptor 2. *J. Biol. Chem.* **287,** 3751–3759
14. Ramsauer, V. P., Carraway, C. A., Salas, P. J., and Carraway, K. L. (2003) Muc4/sialomucin complex, the intramembrane ErbB2 ligand, translocates ErbB2 to the apical surface in polarized epithelial cells. *J. Biol. Chem.* **278,** 30142–30147
15. Le Bivic, A., Quaroni, A., Nichols, B., and Rodriguez-Boulan, E. (1990) Biogenetic pathways of plasma membrane proteins in Caco-2, a human intestinal epithelial cell line. *J. Cell Biol.* **111,** 1351–1361
16. Wang, Z., Yang, H., Ramesh, A., Roberts, L. J., 2nd, Zhou, L., Lin, X., Zhao, Y., and Guo, Z. (2009) Overexpression of Cu/Zn-superoxide dismutase and/or catalase accelerates benzo(a)pyrene detoxification by upregulation of the aryl hydrocarbon receptor in mouse endothelial cells. *Free Radic. Biol. Med.* **47,** 1221–1229
17. Jin, H., Ishikawa, K., Tsunemi, T., Ishiguro, T., Amino, T., and Mizusawa, H. (2008) Analyses of copy number and mRNA expression level of the α-synuclein gene in multiple system atrophy. *J. Med. Dent. Sci.* **55,** 145–153
18. Gomez, G., Townsend, C. M., Jr., Green, D. W., Rajaraman, S., Uchida, T., Greeley, G. H., Jr., Soloway, R. D., and Thompson, J. C. (1990) Protective action of luminal bile salts in necrotizing acute pancreatitis in mice. *J. Clin. Invest.* **86,** 323–331
19. Pasley, J. N., Barnes, C. L., and Rayford, P. L. (1987) Circadian rhythms of serum gastrin and plasma cholecystokinin in rodents. *Prog. Clin. Biol. Res.* **227A,** 371–378
20. Niederau, C., Liddle, R. A., Williams, J. A., and Grendell, J. H. (1987) Pancreatic growth: interaction of exogenous cholecystokinin, a protease inhibitor, and a cholecystokinin receptor antagonist in mice. *Gut* **28,** 63–69
21. Flint, A., Bradwejn, J., Vaccarino, F., Gutkowska, J., Palmour, R., and Koszycki, D. (2002) Aging and panicogenic response to cholecystokinin tetrapeptide: an examination of the cholecystokinin system. *Neuropsychopharmacology* **27,** 663–671
22. Masclee, A. A., Geuskens, L. M., Driessen, W. M. M., Jansen, J. B. M. J., and Lamers, C. B. (1988) Effect of aging on plasma cholecystokinin secretion and gallbladder emptying. *Age* **11,** 136–140
23. Ishibashi, S., Goldstein, J. L., Brown, M. S., Herz, J., and Burns, D. K. (1994) Massive xanthomatosis and atherosclerosis in cholesterol-fed low density lipoprotein receptor-negative mice. *J. Clin. Invest.* **93,** 1885–1893
24. Levy, E., Mehran, M., and Seidman, E. (1995) Caco-2 cells as a model for intestinal lipoprotein synthesis and secretion. *FASEB J.* **9,** 626–635
25. Berna, M. J., Tapia, J. A., Sancho, V., and Jensen, R. T. (2007) Progress in developing cholecystokinin (CCK)/gastrin receptor ligands that have therapeutic potential. *Curr. Opin. Pharmacol.* **7,** 583–592
26. Cawston, E. E., and Miller, L. J. (2010) Therapeutic potential for novel drugs targeting the type 1 cholecystokinin receptor. *Br. J. Pharmacol.* **159,** 1009–1021
27. Yu, L., Bharadwaj, S., Brown, J. M., Ma, Y., Du, W., Davis, M. A., Michaely, P., Liu, P., Willingham, M. C., and Rudel, L. L. (2006) Cholesterol-regulated translocation of NPC1L1 to the cell surface facilitates free cholesterol uptake. *J. Biol. Chem.* **281,** 6616–6624
28. Petersen, N. H., Faegeman, N. J., Yu, L., and Wüstner, D. (2008) Kinetic imaging of NPC1L1 and sterol trafficking between plasma membrane and recycling endosomes in hepatoma cells. *J. Lipid Res.* **49,** 2023–2037
29. Foster, L. J., Li, D., Randhawa, V. K., and Klip, A. (2001) Insulin accelerates interendosomal GLUT4 traffic via phosphatidylinositol 3-kinase and protein kinase B. *J. Biol. Chem.* **276,** 44212–44221
30. Soudah, H. C., Lu, Y., Hasler, W. L., and Owyang, C. (1992) Cholecystokinin at physiological levels evokes pancreatic enzyme secretion via a cholinergic pathway. *Am. J. Physiol.* **263,** G102–G107
31. Chu, B. B., Ge, L., Xie, C., Zhao, Y., Miao, H. H., Wang, J., Li, B. L., and Song, B. L. (2009) Requirement of myosin Vb·Rab11a·Rab11-FIP2 com-

plex in cholesterol-regulated translocation of NPC1L1 to the cell surface. *J. Biol. Chem.* **284,** 22481–22490
32. Welsh, G. I., Leney, S. E., Lloyd-Lewis, B., Wherlock, M., Lindsay, A. J., McCaffrey, M. W., and Tavaré, J. M. (2007) Rip11 is a Rab11- and AS160-RabGAP-binding protein required for insulin-stimulated glucose uptake in adipocytes. *J. Cell Sci.* **120,** 4197–4208
33. Dietschy, J. M., and Turley, S. D. (2002) Control of cholesterol turnover in the mouse. *J. Biol. Chem.* **277,** 3801–3804
34. Gertler, M. M., GARN, S. M., and BLAND, E. F. (1950) Age, serum cholesterol and coronary artery disease. *Circulation* **2,** 517–522
35. MacIntosh, C. G., Andrews, J. M., Jones, K. L., Wishart, J. M., Morris, H. A., Jansen, J. B., Morley, J. E., Horowitz, M., and Chapman, I. M. (1999) Effects of age on concentrations of plasma cholecystokinin, glucagon-like peptide 1, and peptide YY and their relation to appetite and pyloric motility. *Am. J. Clin. Nutr.* **69,** 999–1006
36. Wang, D. Q. (2002) Aging *per se* is an independent risk factor for cholesterol gallstone formation in gallstone susceptible mice. *J. Lipid Res.* **43,** 1950–1959
37. Cheng, Z. J., and Miller, L. J. (2001) Agonist-dependent dissociation of oligomeric complexes of G protein-coupled cholecystokinin receptors demonstrated in living cells using bioluminescence resonance energy transfer. *J. Biol. Chem.* **276,** 48040–48047
38. Cheng, Z. J., Harikumar, K. G., Holicky, E. L., and Miller, L. J. (2003) Heterodimerization of type A and B cholecystokinin receptors enhance signaling and promote cell growth. *J. Biol. Chem.* **278,** 52972–52979
39. Dufresne, M., Seva, C., and Fourmy, D. (2006) Cholecystokinin and gastrin receptors. *Physiol. Rev.* **86,** 805–847
40. Gukovsky, I., Cheng, J. H., Nam, K. J., Lee, O. T., Lugea, A., Fischer, L., Penninger, J. M., Pandol, S. J., and Gukovskaya, A. S. (2004) Phosphatidylinositide 3-kinase γ regulates key pathologic responses to cholecystokinin in pancreatic acinar cells. *Gastroenterology* **126,** 554–566
41. Leevers, S. J., Vanhaesebroeck, B., and Waterfield, M. D. (1999) Signalling through phosphoinositide 3-kinases: the lipids take centre stage. *Curr. Opin. Cell Biol.* **11,** 219–225
42. Rhee, S. G., and Bae, Y. S. (1997) Regulation of phosphoinositide-specific phospholipase C isozymes. *J. Biol. Chem.* **272,** 15045–15048
43. Piiper, A., Stryjek-Kaminska, D., Klengel, R., and Zeuzem, S. (1997) CCK, carbachol, and bombesin activate distinct PLC-β isoenzymes via G_q/11 in rat pancreatic acinar membranes. *Am. J. Physiol.* **272,** G135–G140
44. Scemama, J. L., Robberecht, P., Waelbroeck, M., De Neef, P., Pradayrol, L., Vaysse, N., and Christophe, J. (1988) CCK and gastrin inhibit adenylate cyclase activity through a pertussis toxin-sensitive mechanism in the tumoral rat pancreatic acinar cell line AR 4-2J. *FEBS Lett.* **242,** 61–64